

FOCMEC: FOCal MEChanism Determinations

J. Arthur Snoke

Virginia Tech, Blacksburg, VA, USA

snoke@vt.edu

Abstract

This report accompanies a package for determining and displaying double-couple earthquake focal mechanisms. Input are polarities (P , SV , SH) and amplitude ratios (SV/P , SH/P , SV/SH). The main program, *Focmec*, coded in Fortran 77, performs an efficient, systematic search of the focal sphere and reports acceptable solutions based on selection criteria for the number of polarity errors and errors in amplitude ratios. The search of the focal sphere is uniform in angle, with selectable step size and bounds. The selection criteria for both polarities and angles allow correction or weightings for near-nodal solutions. Applications have been made to finding best-constrained fault-plane solutions for suites of earthquakes recorded at local to regional distances (e.g., Chapman *et al.*, 1997), analyzing large earthquakes observed at teleseismic distances (Snoke, 1990), and using recorded polarities and relative amplitudes to produce waveform synthetics (James and Snoke, 1994).

Program *Focmec* produces two output files: a complete summary of information about all acceptable solutions, and a summary file which can be used as an input to other programs for further analysis or display. Another program in the package, *Focplt*, produces focal-sphere plots based on the *Focmec* summary file of input data (polarities and ratios) alone or superimposed on solutions (fault planes, compression and tension axes, SV and SH nodal surfaces). Other auxiliary programs include one to create input files for program *Focmec*, a program which converts from among various ways of presenting a double-couple solution, a program which calculates the radiation factors for an input mechanism, and programs for displaying and printing plot files.

Instructions are included for compiling and running the programs, and there are two data sets with scripts and documentation for running the programs on the Sun (Unix) platform.

I. Introduction and Overview

Given excellent station coverage for an earthquake in a region for which the earth (seismic velocity) structure was well determined, and with well recorded, impulsive P -wave first arrivals, one could get a reliable estimate for the fault-plane solution (focal mechanism) for the event. More typically, the station density is low, the velocity structure known only approximately, and the polarities of the first arrivals are often ambiguous. It is almost always possible to find up to several focal mechanisms consistent with the data. Generally, the poorer the data, the larger the number of possible solutions. The range of possible solutions can often be further constrained if one can read, to within 10%, the P and S amplitudes on vertical-component seismograms. If one has data from three-component seismographs, the SH to P amplitude ratio provides what could be considered almost independent data. For some

events, one may observe clear SH and/or SV polarities at one or more stations, and the SV/SH amplitude ratio may be better constrained than a ratio including P .

The first version of program *Focmec* was written in 1984 (Snoke, 1984), and since then advances in both seismology and computer technology have led to the introduction of routine determinations of the full moment tensor using digitally recorded waveforms (e.g., Dziewonski, *et al.*, 1981; and Sipkin, 2001). However, these techniques can generally be applied only to large earthquakes recorded at teleseismic distances or at regional distances for earthquakes large enough to have well-recorded surface waves (Randall *et al.*, 1995; Dreger *et al.*, 2000). Programs such as *Focmec* are still the best tools for getting focal mechanisms at local to regional distances, and, for the Sakhalin Island event discussed below, such programs can provide useful insights about the focal mechanism for large events.

The source code included with the distribution of this package has been compiled and linked by the author on a Unix (Sun) platform, but efforts have been made to minimize platform dependence. The plotting routines use the SAC graphics package (see below). All calls in the higher-level routines in this package use generic CALCOMP calls to facilitate adaptation to other plotting packages.

The next section in this report has a discussion of the programming procedure and data preparation. The following section has a description of the programs which make up the package plus some comments on downloading, compiling, and linking them. The final section includes descriptions, input, and output for sample runs. Appendix A contains detailed instructions on how to prepare an input file for program *Focmec*. Appendix B contains definitions of terms used when discussing focal mechanisms. *readme* files, which contain additional details regarding running the programs, are included with the distribution.

When other files in the distribution are mentioned below, their location is given relative to the top directory in the distribution. For example, `./sample_runs/sakhalin/` is the subdirectory containing the drivers, input files, and output files for sample runs involving the Sakhalin Island event, and a copy of this documentation is `./doc/focmec.pdf`.

II. Programming Procedure, and Data Preparation

A. Programming Procedure

The data (station identifiers, azimuths, takeoff angles at the source, polarities, and/or amplitude ratios from among P , SV , and SH arrivals) are read in from a file and stored. Selection parameters are entered through run-time prompts, or from user-customized script files. These include the number of allowed polarity errors for a solution, an acceptable range for deviations between the observed and calculated amplitude ratios, the number of ratio errors that are allowed to be outside that range, the region of the focal sphere to be searched for acceptable solutions and the fineness/coarseness of the search. Using these search criteria, program *Focmec* systematically tests all possible focal mechanisms and lists those that fit the selection criteria. It stores these “possible” mechanisms in two files: a short file with one line per solution which can later be used as an input file for a plotting program, such as *Focplt*, and a more complete listing file which includes four representations of the solutions (dip, strike, rake for either possible fault plane; the **A** and **N** axes trends and plunges, the **P** and **T** trends

and plunges; and the moment tensor), the station identifiers for those with a polarity error, and complete information on the calculated and theoretical amplitude ratios for each station. The conventions used are as in *Aki and Richards* (1980, pp. 105–119) and *Herrmann* (1975), except that our **A** and **N** axes correspond to Herrmann’s **X** and **Y** axes. (See Snoke (1989) for a review of the terminology and conventions related to focal mechanism determinations.)

Two sets of input parameters deserve special mention: relative weighting for polarities, and, for ratios, *P* or *S* “cutoffs” when the numerator or denominator radiation factor is near a nodal surface.

The default polarity weighting is unity, so one gets a “1” for every modeled polarity that does not match the observed polarity. A program alternative is to use weighted polarities, for which case a near-nodal radiation factor mismatch will count for less than one near the middle of the quadrant.

If the numerator or denominator radiation factor is near a nodal surface, the result is a large amplitude for the calculated $\log_{10}(\text{ratio})$. Further, the velocity structure may not be so well constrained that polarity errors near a nodal surface should be rejected. If the factor is less than the chosen cutoff, it gets replaced by the cutoff when calculating the ratio. Flags in the complete-solution output file indicate if the numerator, denominator, or both were below the cutoffs and to let the user know that those ratios may have to be examined more closely.

B. Data Preparation

The convention for the takeoff angle is that 0° is down. The polarity convention and the notation for amplitude ratios are included in Appendix A. For phases to be used in an amplitude ratio, an implicit assumption is that the source process is simple and the travel paths similar (negligible multipathing). If the frequency content is essentially the same and the seismometers on which they are recorded are matched, one can use the raw traces. Before using *SV* data, read Appendix C below. In general, if one has 3-component data, polarities and ratios involving *SH* are the more likely to be estimated with much confidence.

For calculating focal mechanisms from polarities, one needs event-based azimuths and takeoff angles for each phase from the source. If one uses amplitude ratio data, one needs the emergence angles for free surface corrections, and, if a correction for attenuation is to be used, the travel times for the phases used. These data are generally provided along with the event locations – e.g., from an earthquake-location program such as *Hypoellipse* (Lahr, 1999). If so, one could write a program (such as program *Hypo2foc* provided with this package) to take such data from the earthquake-location output file and put it directly into a *Focmec* input file. Programs *Fileprep* and *Fmecprep*, also included with this package and discussed below, provide an alternative procedure to prepare a *Focmec* input file. Finally, one could simply enter the data by hand, using the *Focmec* input-file format outlined in Appendix A.

For crustal events recorded at local or regional distances, the first arrivals may be the refracted phases *Pn* and *Sn*. If the Poisson’s ratio is constant in the crust and uppermost mantle, *Pn* and *Sn* will leave from the same point on the focal sphere and have identical travel paths, so their ratio can be used.

III. Programs

A. Program *Focmec*

Program *Focmec* is the mainline program in the package. It requires one input file which contains the ratio and polarity data for a single earthquake. All other input can be done interactively or from a script. See the subdirectories of *./sample_runs/* for examples of both input files (called *focmecXXX.inp*) and scripts (*rfocmecXXX*). Output is two files, a listing file containing detailed information about each acceptable solution (*focpltXXX.lst*) and an output file with a header summarizing the data and run parameters followed by a single line per solution (*focmecXXX.out*). This second file can be used as input for a plotting program which displays data and/or solutions.

The source for the program is in *./src/*. It includes comments summarizing the modification history for the package. Before compiling and linking the program, one must build the library *libfm.a*. The sources for the subroutines and the (Unix) makefile are in directory *./fm-sub/*, and the library is placed in *./lib/*. The executable for this program is put in directory *./bin/*.

B. Data-Preparation Programs

This package contains two programs to assist in the preparation of *Focmec* input files. The first, *Fileprep*, takes as its input a hypocenter plus a list of stations for which it calculates epicentral distances and azimuths. Using the *iasp91* velocity model and traveltimes tables (Kennett and Engdahl, 1991), it calculates takeoff and emergence angles for both *P* and *S* as well as first-arrival *P* and *S* arrival times. The output file is one line per station, which is then read by the companion program *Fmecprep*. Program *Fmecprep* also reads in an event-specific file with one line for each polarity or ratio. For polarities, it reads in the station name and the polarity-ratio key (see Appendix A). As of March 2002, emergent arrivals for which the user assigns a polarity can be used if desired. For a ratio, the line has the station, the ratio key, the key for the polarity of the numerator (not used, but displayed in the complete listings), and either two or six numbers separated by commas — the numerator and denominator amplitudes plus (if used) attenuation data in the form Q_{num} , Q_{den} , freq_{num} , freq_{den} , where the “freq” terms are the frequencies at which the amplitudes were determined. (If an amplitude for *SV* is used, *Fmecprep* assumes it is from the radial component. If it was measured on the vertical, it must be converted: program *Freesurf* can be used to calculate the correction term.) The output of *Fmecprep* is a file which can be used as the data input file for program *Focmec*.

As noted above, program *Hypo2foc*, provided with this package, is an example of a program for preparing a *Focmec* input file from an earthquake-location program output file. (See file *focmec-doc/readme_etnevent.html*.) An additional program will be needed if one is to include amplitude-ratio data.

The *iasp91* traveltimes tables and velocity model are in directory *./iasp91stuff/*, and the station location file used for one of the sample runs is in directory *./sample_runs/*. To compile and link the programs, one goes to the source directory and uses the *cl* command. For program *Fileprep*, an additional library is needed: *libiasp91.a*. This is created by entering the command *make* in directory *./iasp91stuff/*. This library is not needed for program *Fmecprep*.

C. Other Analysis Programs

Three subsidiary analysis programs are included: *Solsort*, *DSRetc*, and *Radiat*. Source (.f) files are in the *./src/* directory, and the programs can be built using *./src/cl* after the library *libfm.a* has been built. No plotting is involved in any of these. To run them, just enter the program name and respond to the prompts. No other input is required.

- *DSRetc* allows one to convert from among the various ways to represent a focal mechanism — dip, strike, rake; plunge/trend for **P** and **T** or **A** and **N**; and the moment tensor representation (for a mechanism which has a significant double-couple component). Also included is a beach-ball printer plot showing the *P*-wave nodal planes (Sipkin, 1993, personal communication. He gives credit to Bob Uhrhammer.)
- *Radiat* produces radiation factors and amplitude ratios for input dip, strike, rake, takeoff angle, and azimuth.
- *Solsort* (compliments of Rick Williams, but not used much by me . . .) allows one to take the output file from *Focmec* (.out file) and select by several criteria subsets of solutions.
- *Freesurf* helps one figure out free-surface corrections for ratios.

D. Plotting Program

Program *Focplt* is the plotting program in the *Focmec* package. Input can be from *Focmec* input (for data) or output files (for solutions). The plots are equal-area Lambert-Schmidt projections (usually lower hemisphere) of the focal sphere. Plots can include any or all from among the following: the data, fault planes, **P**, **T**, **B** axes, and *SV* or *SH* nodal surfaces for solutions. There are options for adding time stamps a title, and labels. The program can be run interactively or from a script. Programs are also included which allow one to display output plot files on the screen (*sgfp*) or convert them to postscript files (*sgf2ps*). Further information on how to use these programs is included in *focmec-doc/readme_etnevent.html*.

E. Downloading, Compiling, and Linking the Programs

The *Focmec* software package including sources, documentation, and examples is in a compressed .zip files (PKZIP format): *focmec_pkg.zip*. (Utilities exist for most platforms and operating systems which can “unzip” .zip files. If you don’t have one on your system, you can probably find one at URL <http://www.info-zip.org/>.) Executables for current versions of all programs are included for *Sun Solaris 2.8* (*focmec_sol-binlib.zip*) and for all programs as of June 2000 on *Sun Sunos 4.1.4* (*focmec_sun-binlib.zip*). Also included are PC versions (Windows 98 or later) of sources and executables for current versions of all programs except the plotting program *Focplt*; sources are in the software package file in directory *./src-PC/*, executables are in *focmec_exe-PC.zip*. (For Unix users who do not have the *zip/unzip* utilities but do have *tar* and the GNU *gzip* utility, the software package and the two *binlib* files are also stored on the server in *gzip*-compressed *tar* format. The single command *gzip -d -c focmec_pkg.tgz | tar -xf -* will uncompress the input file and un-tar it while leaving the input file unchanged.)

The evolutionary history of the software package includes versions which ran on IBM Mainframe, PDP/RSX, VAX/VMS, Sun snuos, Sun Solaris. As written, the programs can be compiled and will run on a Unix Sun Sparcstation (Sunos 4.1.x, and/or Solaris 2.x). The Sun F77 compiler was used for all Fortran programs, and the GNU GCC compiler was used for the one C auxiliary program. Attempts have been made to make the code as platform independent as possible. Statements related to opening and closing files often depend on the operating system and compiler, as would the (non-essential) routines which return the time and date. The readme files included in the package have further details.

Occasionally corrections, updates, or enhancements are made to parts of the package. These will be available at URL <http://www.geol.vt.edu/outreach/vtso/focmec/>, the site for the Web-based version of the package, and any changes will be documented in the update-history page on that server — which as of this writing is the same as *focmec-doc/update.html*.

Sources are included for all programs and subroutines except those in the SAC library, which are used only if SAC graphics is implemented in program *Focplt*. The plotting programs use the Lawrence Livermore National Lab (LLNL) graphic routines developed for their Seismic Analysis Code (SAC). In the mid 90s, LLNL rewrote their analysis package and renamed it SAC2000 (Goldstein *et al.*, 1998; Vergino and Snoke, 1993). The “front end” routines called by program *Focplt* are based on the pre-SAC2000 package and require a Fortran subroutine library, which is available for many platforms from the authors of SAC2000. (The Sun Sunos and Sun Solaris versions of this library are included with the FOCMEC executables which can be downloaded from the FOCMEC Web site.) In addition to needing this library, one must also run the makefile in directory *./fplotsub/*, to create the library *./lib/libfplotsub.a*. There are scripts in *./src/* to compile and link the programs, putting the executables in *./bin/*. See *readme_focmec.html* for further details.

Recently (January 2003) I wrote a set of Fortran subroutines which can create SAC Graphics Format (SGF) files with no calls to the SAC Fortran library. See *readme_focmec.html* for further discussion about creating, displaying, and converting plot files.

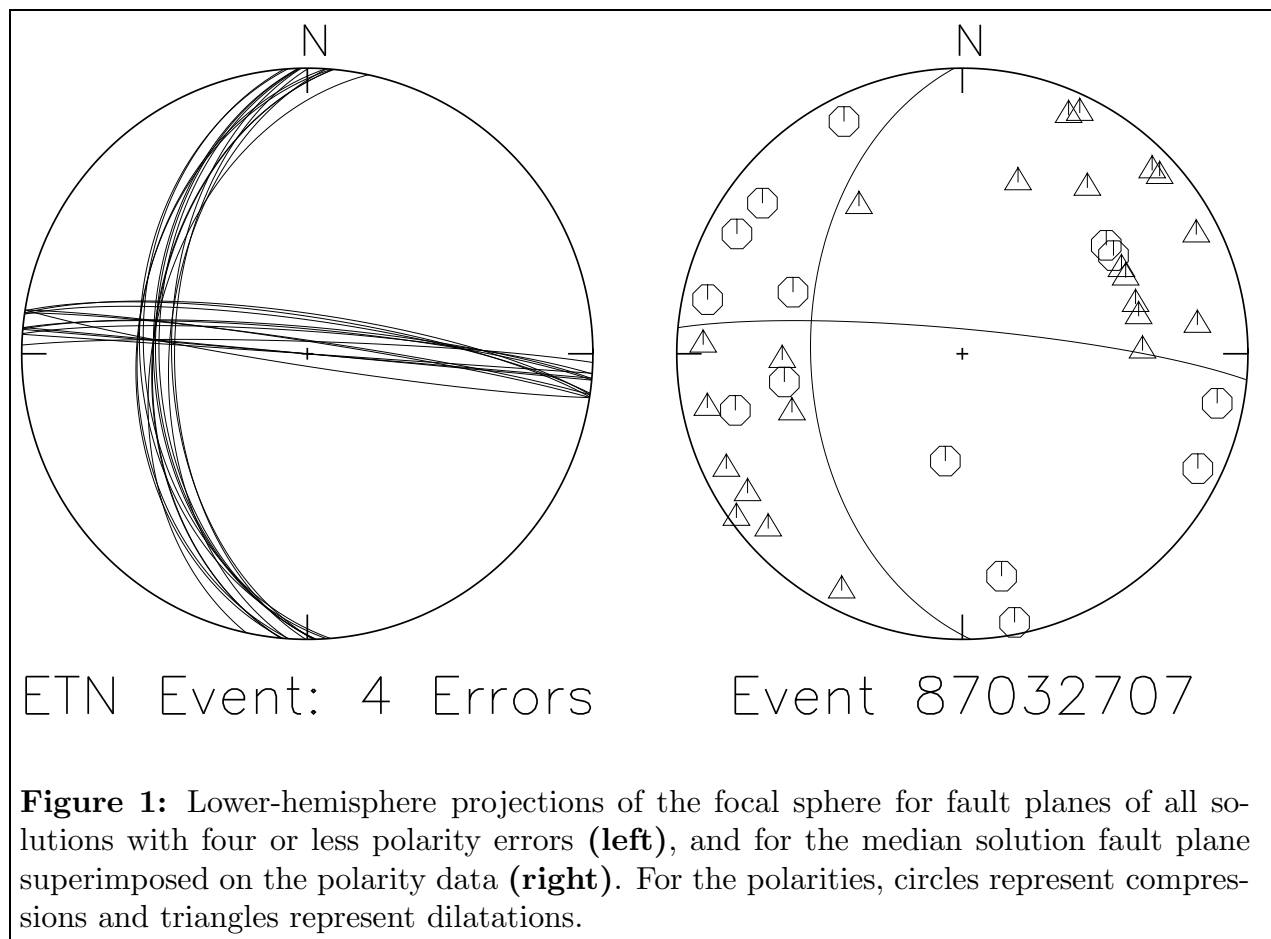
IV. Sample Runs

Directory *./sample_runs/* has in turn two subdirectories which have real-data applications of the *Focmec* package. The first is for a magnitude 4.2 earthquake with a focal depth of 19 km recorded by stations for which *P*-wave polarity data were available from 38 stations at local to regional distances. The second example is the 1990 M=6.5 deep-focus (611 km) Sakhalin Island event. For this event, a dataset of 190 *P*-wave polarity recorded at teleseismic distances is compared with an enhanced data set which includes polarities for *SV* and *SH* along with amplitude ratios recorded at eight broadband stations. For each event, there is a readme file in directory *./sample_runs/*.

A. Eastern Tennessee Event

Directory `./sample_runs/ETNEvent` includes drivers, input, and output files for an application of the *Focmec* package to a magnitude 4.2 event with a focal depth of 19 km which occurred on 27 March 1987 in eastern Tennessee and was recorded by regional networks on short-period, vertical-component seismographs. Only *P* polarities were used to determine the focal mechanism. This event is number 12 in Chapman *et al.* (1997).

The input file includes direct-*P* arrival polarity picks for 38 stations. The azimuths and takeoff angles were produced by the earthquake location program (*Hypoellipse*), and the *Focmec* input file was created using program *Hypo2foc*. The results presented here are for allowing up to four fixed-weight polarity errors. Using relative weighting for the errors did not improve the solution. Plots produced by program *Focplt* are shown in Figure 1.



B. Sakhalin Island Event

The 12 May 1990 $M=6.5$ $z=611$ km Sakhalin Island event, which is the only deep-focus event in the NOAA/NEIC catalog within about 200 km of its epicenter at 49.02°N and 141.94°E . In 1990 a GSETT-2 broadband seismograph was installed in Blacksburg, and the IRIS fast-retrieval system (then called “Gopher”) was fairly new, so the author did an analysis of this event both as a training tool on seismographs and data retrieval and also as a test of the capabilities of the *Focmec* package. Results of this study were presented at the October 1990 Eastern Section of the SSA meeting held in Blacksburg (Snoke, 1990). Directory `./sample_runs/sakhalin` includes drivers, input, and output files for an update of that study. Included are runs of programs *Fileprep* and *Fmecprep* to find the azimuths, takeoff angles, and \log_{10} amplitude ratios for a *Focmec* input file which contains both polarity and amplitude ratio data. Also included are *Focmec* runs comparing solutions based on only *P*-wave polarities and an enhanced data set using *S*-wave polarities and amplitude ratios. The best solutions for these two data sets are significantly different, and the solution based on the enhanced data set is identical to the best double-couple Harvard CMT solution. (This 1990 study contributed to the realization that the vertical component at station HRV and all three components at station KIP had reversed polarities.)

For the 1990 presentation, there was a database of seven IRIS-reporting stations plus BLA, including instrument response (which allowed accurate determinations of the radial and transverse directions and amplitude ratios), along with the NEIC preliminary *P*-wave polarity data base with picks for 190 stations. The station distribution can be seen in the left-hand panel in Figure 2, with larger symbols indicating the eight broadband, three-component stations. As is often the case for large, deep-focus earthquakes, the body-wave arrivals were impulsive with simple waveforms, allowing reliable polarity picks and measurements of amplitudes. (These waveforms, along with those from many additional stations, can now be gotten from the IRIS Data Management Center “FARM” database.)

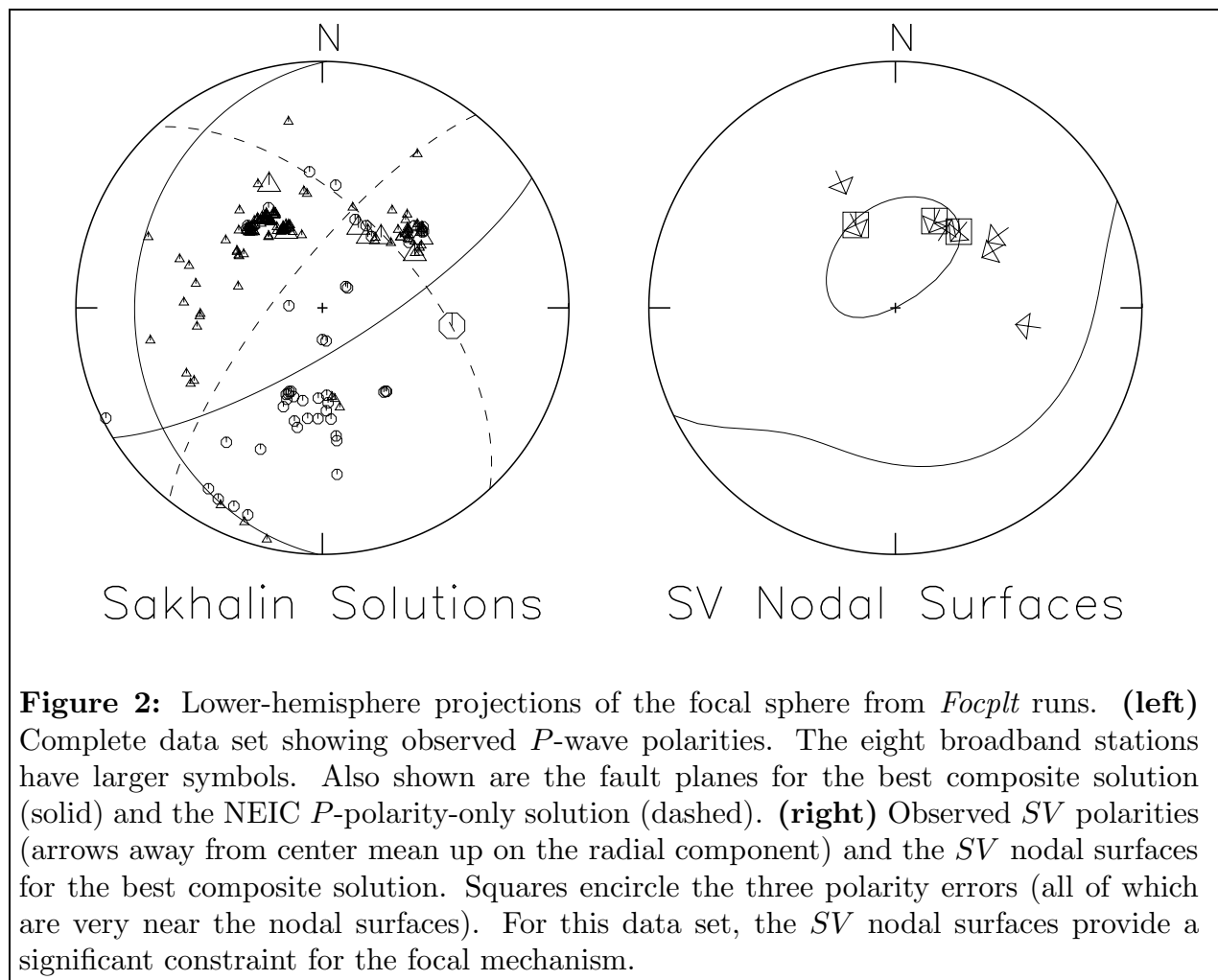
The NEIC database and the 1990 analysis of the eight broadband stations used the JB velocity model and traveltime tables to calculate takeoff angles and, for the amplitude ratios, the free-surface corrections. For the runs included with this package, the *iasp91* velocity model and traveltime tables were used to allow demonstrations of programs *Fileprep* and *Fmecprep* for the broadband stations. The differences in takeoff angle are never more than a couple of degrees which lead to negligible differences in the *Focmec* solutions. (Not done here is any fine-tuning of the free-surface corrections for individual stations, but, using the supplementary program *Freesurf*, it would be easy to modify the input for program *Fmecprep*.)

Program *Fileprep* takes as input the earthquake hypocenter and set of stations along with the *iasp91* velocity model and traveltime tables. Its output file contains angles and travel times for each station. Program *Fmecprep* takes the output file from *Fileprep* as well as a file which has the event data: station, polarity or ratio key, plus further information if the key is for a ratio. The output file from *Fmecprep* can be used as an input file for program *Focmec*.

Amplitudes used for amplitude ratios are calculated at the source. At higher frequencies *S* waves lose amplitude relative to *P* waves because of attenuation, so one must correct for the relative attenuation for amplitude ratio analysis. For these data, amplitudes were measured on matched records for low-pass filtered settings with corners at 0.1 Hz and 0.01 Hz (Butterworth

4 pole) and found very small differences, so no correction was used for attenuation in the 1990 study. For completeness, a *Fmecprep* run is included which has corrections for attenuation in the S/P ratios.

SV arrivals are picked on the radial component. For two of the stations, BLA and HRV, phase SKS arrived within ~ 20 seconds before direct S . If low-pass filtering is used on the radial component, SKS interferes with S resulting in a lack of accuracy in estimating the SV amplitude. For these two stations, SV/P ratios were not used, rather, SV/SH which were estimated using amplitudes measured on the unfiltered radial seismograms – for which there was no interference between SKS and S on the radial components.



The best fit for the NEIC P -polarity data set had 20 errors out of the 190 picks. (Allowing for 22 errors produced a set with very little spread, so the solution seemed stable.) Using the relative-error option with a threshold of 0.1 for solution errors produced essentially the same set of solutions.

Adding in the polarity plus amplitude-ratio data from the eight broadband stations changed the solution from the best-fit NEIC P -polarity solution. The included *Focmec* run is for the minimum number of errors assuming no ratio errors (among the 16 from the eight stations) with an acceptable error of 0.50 for the \log_{10} ratio, and 27 allowed errors among the 197 P polarities, 8 SV polarities, and 8 SH polarities (station TOL had been included in the NEIC data set). An effectively equivalent set of solutions results from a relative-error run with 15 allowed errors with a threshold of 0.1. The best composite solution is the same as the final Harvard CMT solution of 75.92° , 58.18° , and -69.35° for the dip, strike, and rake. This is not surprising, in that the CMT solution used data from all these stations — except perhaps BLA. But it shows that a solution using just polarities and amplitude ratios can do as well — at least in this case — as a solution based on full waveform inversion for the best constrained double-couple solution. (One can see all the official final solutions on the ISC web page by using a time-location event sort.) The left-hand panel in figure 2 shows the data and comparisons between the different solutions. The right-hand panel shows explicitly how, for this data set, the SV arrivals constrain the solution.

It is interesting to see how solutions based on all the data compare with the preliminary NEIC solution. To test this, one uses the complete data set but restricts the focal-sphere search to the single solution. In the run for program *Focmec*, one relaxes the bounds for an acceptable solution so the desired solution is not rejected. The files containing the string *all-neicF* in their filenames are the input and output files for this run. From the eight additional stations, one finds that the preliminary NEIC solution has four more P polarity errors, six SV polarity errors, six SH polarity errors and ten ratio errors.

A more complete analysis of this event would include runs of *Focmec* with more errors allowed to show how well constrained the final solutions are. Also, the seismograms for KEV (at 54.58°) show numerous arrivals between P and S : PcP pP , sP , ScP , and sPP . The *iasp91* package gives arrival times and takeoff angles for all these phases, so in principle, these polarities could be used as additional input to program *Focmec* — after allowing for any polarity flips on reflection or conversion. If such arrivals are well recorded, one could use amplitude ratios from among them, but one would have to add in conversion/reflection coefficients. (Also, if there is significant directivity for the event, one may need to consider implications of differences in takeoff angles for the two rays.)

V. References

- Aki, K. and P. G. Richards (1980). **Quantitative Seismology: Theory and Methods**, W.H. Freeman, San Francisco, CA.
- Booth, D. C. and S. Crampin (1985). Shear-wave polarizations on a curved wavefront at an isotropic free surface, *Geophys. J. R. astr. Soc.*, **83**, 31–35.
- Chapman, M. C., C. A. Powell, G. Vlahovic and M. S. Sibol (1997). A statistical analysis of earthquake focal mechanisms and epicenter locations in the eastern Tennessee seismic zone, *Bull. Seism. Soc. Am.*, **87**, 1522–1536.

- Dreger, D. S., H. Tkalčić, M. Johnston (2000). Dilational processes accompanying earthquakes in the Long Valley Caldera, *Science*, **288**, 122–125.
- Dziewonski, A. M., T. A. Chou, and J. H. Woodhouse (1981). Determination of earthquake source parameters from waveform data for studies of regional and global seismicity, *J. Geophys. Res.*, **86**, 2825–2852.
- Goldstein, P., D. Dodge, M. Firpo, and S. Ruppert (1998), What's new in SAC2000? Enhanced Processing and Database Access, *Seism. Res. Letters*, **69**, 202–204
- Gubbins, D. (1990). **Seismology and Plate Tectonics**, Cambridge University Press, Cambridge
- Herrmann, R. B. (1975). A student's guide for the use of P and S wave data for focal mechanism determination, *Earthquake Notes*, **46/4**, 29–39.
- James, D. E. and J. A. Snoke (1994). Structure and tectonics in the region of flat subduction beneath central Peru. Part I: Crust and uppermost mantle: *J. Geophys. Res.*, **99**, 6899–6912.
- Jost, M. L. and R. B. Herrmann (1989), A student's guide to and review of moment tensors, *Earthquake Notes*, **60/2**, 37–57.
- Kennett, B. L. N., and E. R. Engdahl (1991). Traveltimes for global earthquake location and phase identification, *Geophys. J. Int.* **122**, 429–465. The 1996 release can be gotten from the USGS site <ftp://ghftftp.cr.usgs.gov/pub/tau/experimental/tau.tar.Z>. Source code for other operating systems are included in [/pub/tau/](#).
- Kisslinger, C. (1980). Applications of S to P amplitude ratios for determining focal mechanisms from regional network observations, *Bull. Seism. Soc. Am.*, **70**, 999–1014.
- Kisslinger, C., J. R. Bowman, and K. Koch (1981). Procedures for computing focal mechanisms from local (SV/P) ratios, *Bull. Seism. Soc. Am.*, **71**, 1718–1729. Correction for both this and the preceding paper was published in *BSSA* volume **72** on page 344.
- Kisslinger, C., J. R. Bowman, and K. Koch (1982). Determination of focal mechanisms from (SV/P) amplitude ratios at small distances, *Phys. Earth and Planet. Inter.*, **30**, 172–176.
- Lahr, J. C. (1999), HYPOELLIPSE Y2K: A computer program for determining local earthquake hypocentral parameters, magnitude, and first-motion pattern, U.S. Geological Survey Open-file Report 99–023, 112p. On-line: <http://greenwood.cr.usgs.gov/pub/open-file-reports/ofr-99-0023>. http://geohazards.cr.usgs.gov/iaspei_pgms/hypoellipse/ is the URL for the current version of the package, including documentation and executables for both PC and Sun/Unix.

- Randall, G. R., C. J. Ammon and T. J. Owens (1995). Moment-tensor estimation using regional seismograms from a Tibetan Plateau portable network deployment, *Geophys. Res. Letters*, **22**, 1665–1668.
- Sipkin, S. A. (2001). USGS Moment tensor software and catalog, this volume.
- Snoke, J. A., J. W. Munsey, A. C. Teague, and G. A. Bollinger (1984), A program for focal mechanism determination by combined use of polarity and *SV-P* amplitude ratio data, *Earthquake Notes*, **55**, #3, 15.
- Snoke, J.A. (1989). Earthquake Mechanisms, **Encyclopedia of Geophysics** (D. E. James, Ed.), Van Nostrand Reinhold Company, New York, 239–245.
- Snoke, J.A. 1990, Clyde and the Gopher: a preliminary analysis of the 12 May 1990 Sakhalin Island event, *Seism. Res. Letters*, **61**, 161.
- Stein, S. and E. Klosko (2002), Earthquake Mechanisms and Plate Tectonics, **International Handbook of Earthquake and Engineering Seismology** (W. H. K. Lee, H. Kanamori, P. C. Jennings, and C. Kisslinger, Eds.), Academic Press, San Diego, Chapter 7.
- Vergino, E. and J. A. Snoke (1993). SAC and MAP, *IRIS Newsletter*, **XII.2**, 7–9.

Appendix A: Input conventions and format for *Focmec* and *Focplt*

This is a text file describing the input format for *Focmec* (done in subroutine *focinp.f*) and which is used in program *Focplt* (through subroutine *prplot.f*) for displaying first motions and/or ratios.

```

      READ(1,'(A)') COMMNT ! First line input file
200   READ(1,5,END=300,ERR=500) STA,AZIN,TOANG,SENSE,
      .   RATLOG,SVSH2,STOANG,INFO
5     FORMAT(A4,2F8.2,A1,F8.4,1X,A1,1X,F6.2,1X,A)

```

- STA is a name for the station. Up to four characters. Not used
- AZIN is the azimuth (degrees) of the station measured from the epicenter
- TOANG is the takeoff angle (degrees) of the *S* if *S* polarity or a *SV/P*, *SH/P*, or *SV/SH* ratio. It is a *P* takeoff angle for a *P* polarity
- SENSE is a one-character key for a polarity or a ratio

Virginia Tech Symbol conventions:

- C = compression at station (plotted as a hexagon symbol number NS = 1)
- U = same as C (up on vertical)

D = dilatation --- down on vertical (plotted as a triangle NS=2)
 + = emergent compression (NS=3) (optionally included in Focmec)
 - = emergent dilatation (optionally included in Focmec)
 e = emergent P arrival
 > = SH first motion to right (back to event, facing station) impulsive
 < = SH first motion to left (back to event, facing station) impulsive
 L = same as <
 R = same as > (Note: earlier versions used R for SV/P ratio)
 F = SV first motion away from event impulsive
 B = SV first motion towards event impulsive
 The SH and SV first motions are plotted as oriented arrows (NS=6)
 l = SH first motion to left (back to event) emergent
 r = SH first motion to right (back to event) emergent
 u = emergent SH arrival
 V = Log10(SV/P) (NS=4) (plotted as an X)
 H = Log10(SH/P) (NS=4) (plotted as an X)
 S = Log10(SV/SH) (NS=4) (plotted as an X)

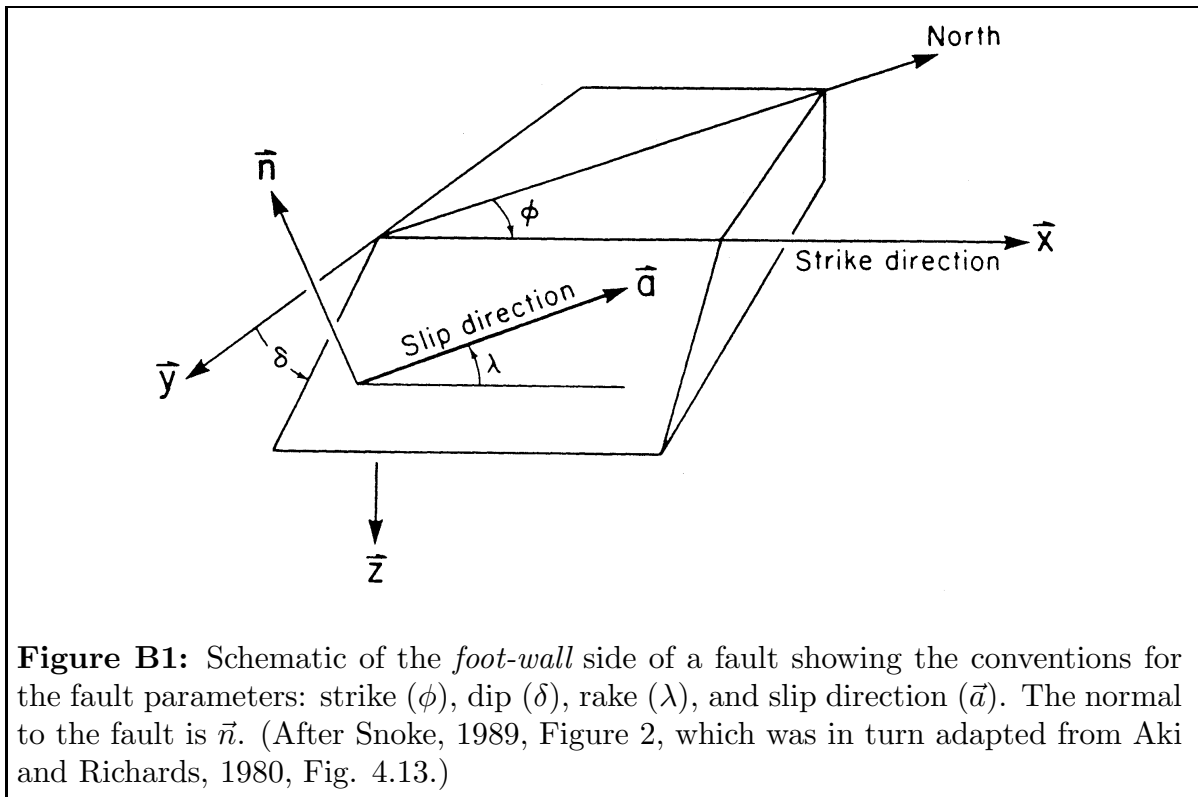
If one wants to have errors marked, follow the polarity or ratio with a duplicate line with an E in the symbol position. The error will then be flagged by a square superimposed on the polarity or ratio. If SENSE is R, V, or H:

- RATLOG is the $\log_{10} (S/P)$
- SVSH2 is the polarity of numerator S . It is not used, but is shown in the listing file along with the calculated values. Convention used for the calculated ones are L and R for SH , B and F for SV
- TOANG1 is the S takeoff angle
- INFO is a field of up to 40 characters. If the input file was prepared by Fmecprep, it summarizes information used in the amplitude ratio. (See `./sample_runs/sakhalin` for an example.)

No terminator line is needed. MAX in FOCMEC.INC is the maximum number of allowed ratios plus polarities.

Appendix B: Glossary for Focal Mechanisms

Seismic Moment Tensor: The ground displacement from an earthquake can be written as the convolution of a moment tensor and the gradient of a Green's function. The Green's function includes propagation effects, while the moment tensor contains information about the source properties. The moment tensor can be interpreted as the volume integral of the stress release associated with the earthquake. The most general moment tensor has six independent components, but the focal mechanisms for the vast majority of earthquakes are well described by a *double couple*, for which the moment tensor has only three independent components. See Jost & Herrmann (1989) for a comprehensive review of moment tensors.



Strike, Dip and Rake: One way to parameterize a double-couple solution is to specify, with three angles, the direction of a vector along the direction of slip of the earthquake along a fault surface. The **strike** (ϕ) is the azimuth of the fault, with the convention that if one faces down-dip, the strike direction is to the left. The **dip** (δ) is measured down from the horizontal and is bounded by 0° and 90° . The **rake** (λ) is along the direction of slip on the fault surface and is bounded by -180° and $+180^\circ$. The convention for rake angle λ : Reverse fault if $0^\circ < \lambda < 180^\circ$, normal fault if $-180^\circ < \lambda < 0^\circ$, right-lateral strike slip if $\lambda = 180^\circ$, and left-lateral strike slip if $\lambda = 0^\circ$. Note that with \hat{z} down (Figure B1), both $(\hat{x}, \hat{y}, \hat{z})$ and (North, East, \hat{z}) are right-handed coordinate frames.

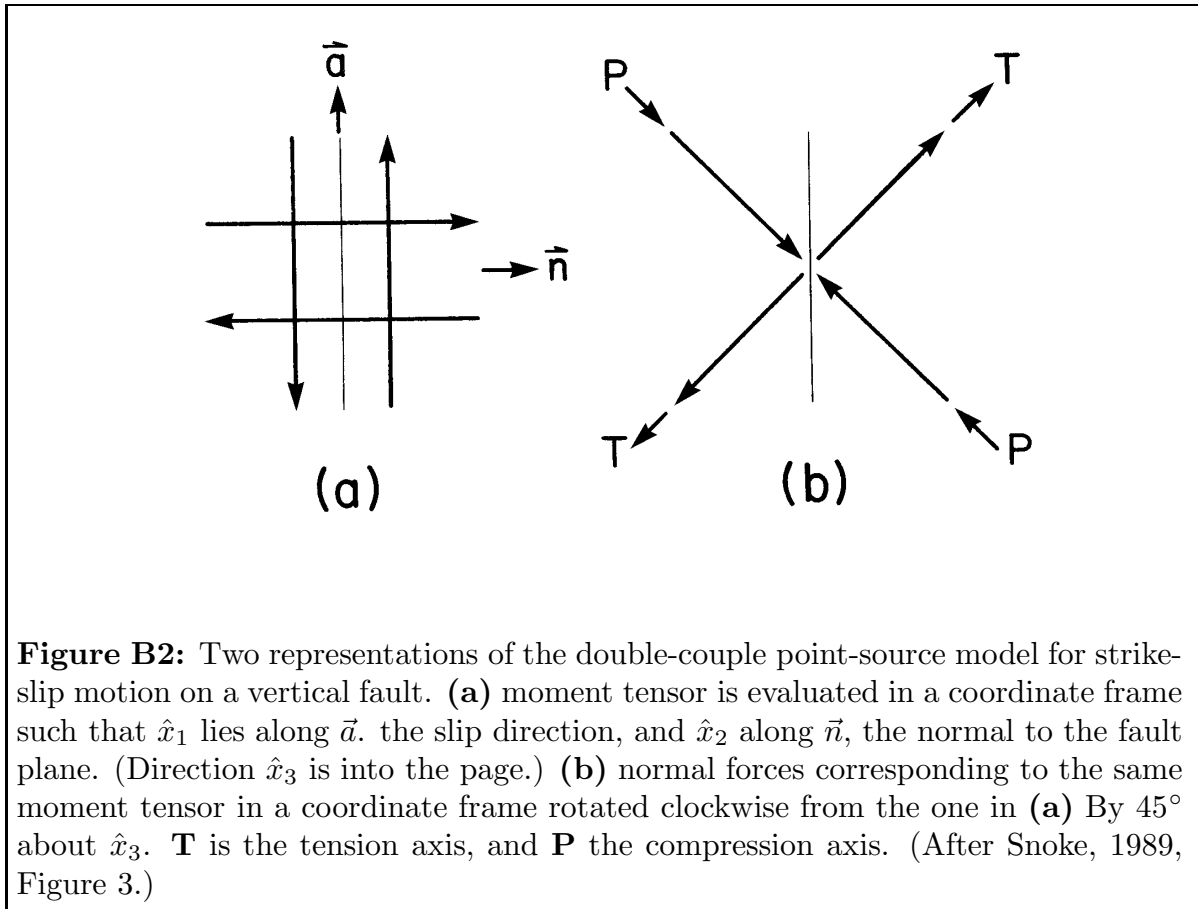
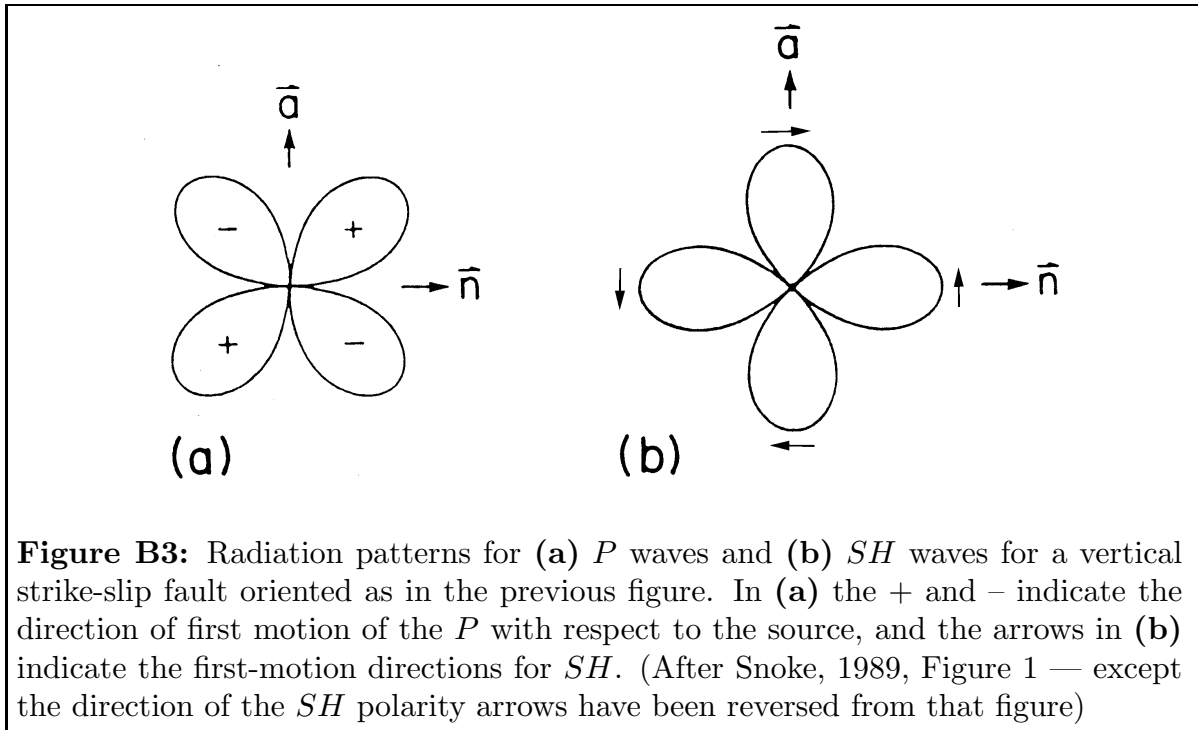


Figure B2: Two representations of the double-couple point-source model for strike-slip motion on a vertical fault. **(a)** moment tensor is evaluated in a coordinate frame such that \hat{x}_1 lies along \vec{a} , the slip direction, and \hat{x}_2 along \vec{n} , the normal to the fault plane. (Direction \hat{x}_3 is into the page.) **(b)** normal forces corresponding to the same moment tensor in a coordinate frame rotated clockwise from the one in **(a)** By 45° about \hat{x}_3 . \mathbf{T} is the tension axis, and \mathbf{P} the compression axis. (After Snoke, 1989, Figure 3.)

Pressure and Tension Axes: As shown in Figure B2, an alternative parameterization for a focal mechanism is to specify the trend and plunge of the \mathbf{P} axis (direction of maximum source compression which is the same as the direction of maximum dilatation at the recording site) and \mathbf{T} axis (direction of maximum source dilatation or recording-site compression). Because the \mathbf{P} and \mathbf{T} axes are orthogonal, there are only three independent parameters from among the two sets of trends and plunges, so there are still only three independent parameters in this representation. This representation for a focal mechanism is particularly useful for relating earthquake mechanisms to directions of compression or tension of the regional stress.

Focal Sphere: Modeling the earthquake as a point source, the focal mechanism can be uniquely specified by specifying the directions of \mathbf{P} and \mathbf{T} with respect to a sphere of vanishingly small radius surround the focus (Figure B2b). Observations of polarities and amplitudes used to constrain the solution must be corrected to points on the focal sphere designated by the takeoff angle and azimuth for the raypath leading to that station.



Radiation Pattern: A double-couple solution produces a radiation pattern for P waves with four quadrants which are alternatively compressive and dilatational. Figure B3 shows the four quadrants for both the P and SH radiation patterns.

Fault Plane and Auxiliary Fault Plane: The radiation patterns for SV and SH have similar four-fold symmetry to that for P , and the result is that there are two equally possible fault planes consistent with all polarity and ratio data for a single event. Hence for each solution, two possible sets of dip, strike and rake are presented, and each fault-plane plot includes two planes. Solutions produced by program *Focmec* include the trend and plunge of vectors \mathbf{A} and \mathbf{N} , which are along the slip directions in the two possible fault planes (\vec{a} and \vec{n} in the preceding two figures in this section). These vectors can be gotten from \mathbf{P} and \mathbf{T} by a rotation of 45° around the vector \mathbf{B} , which is along the normal to the plane formed by \mathbf{P} and \mathbf{T} .

Sign Conventions for Components of Ground Motion: Polarities in the FOCMEC package are designated by directions with respect to an observer facing the station with his/her back to the epicenter. Accordingly, *P* arrival first motions are up or down, *SH* left or right, and *SV* forward or backward.

Horizontal components for a three-component seismograph must be rotated from *North-South* and *East-West* into *Radial* and *Transverse* to separate *SV* from *SH*. The convention in common usage — e.g., in SAC2000 — has positive *Radial* as forward and positive *Transverse* as to the right with respect to an observer facing the station. Note that *Vertical*, *Radial*, and *Transverse* form a left-handed coordinate frame.

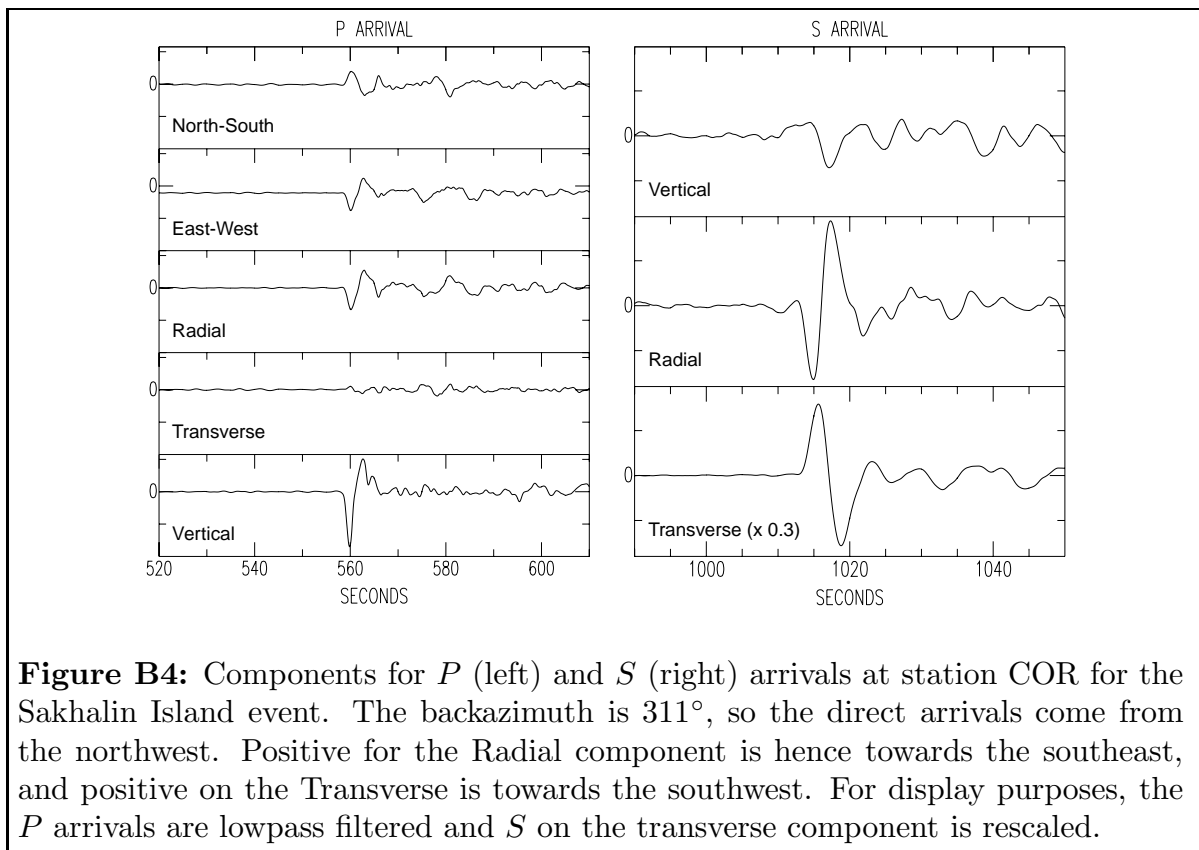


Figure B4: Components for *P* (left) and *S* (right) arrivals at station COR for the Sakhalin Island event. The backazimuth is 311° , so the direct arrivals come from the northwest. Positive for the *Radial* component is hence towards the southeast, and positive on the *Transverse* is towards the southwest. For display purposes, the *P* arrivals are lowpass filtered and *S* on the *transverse* component is rescaled.

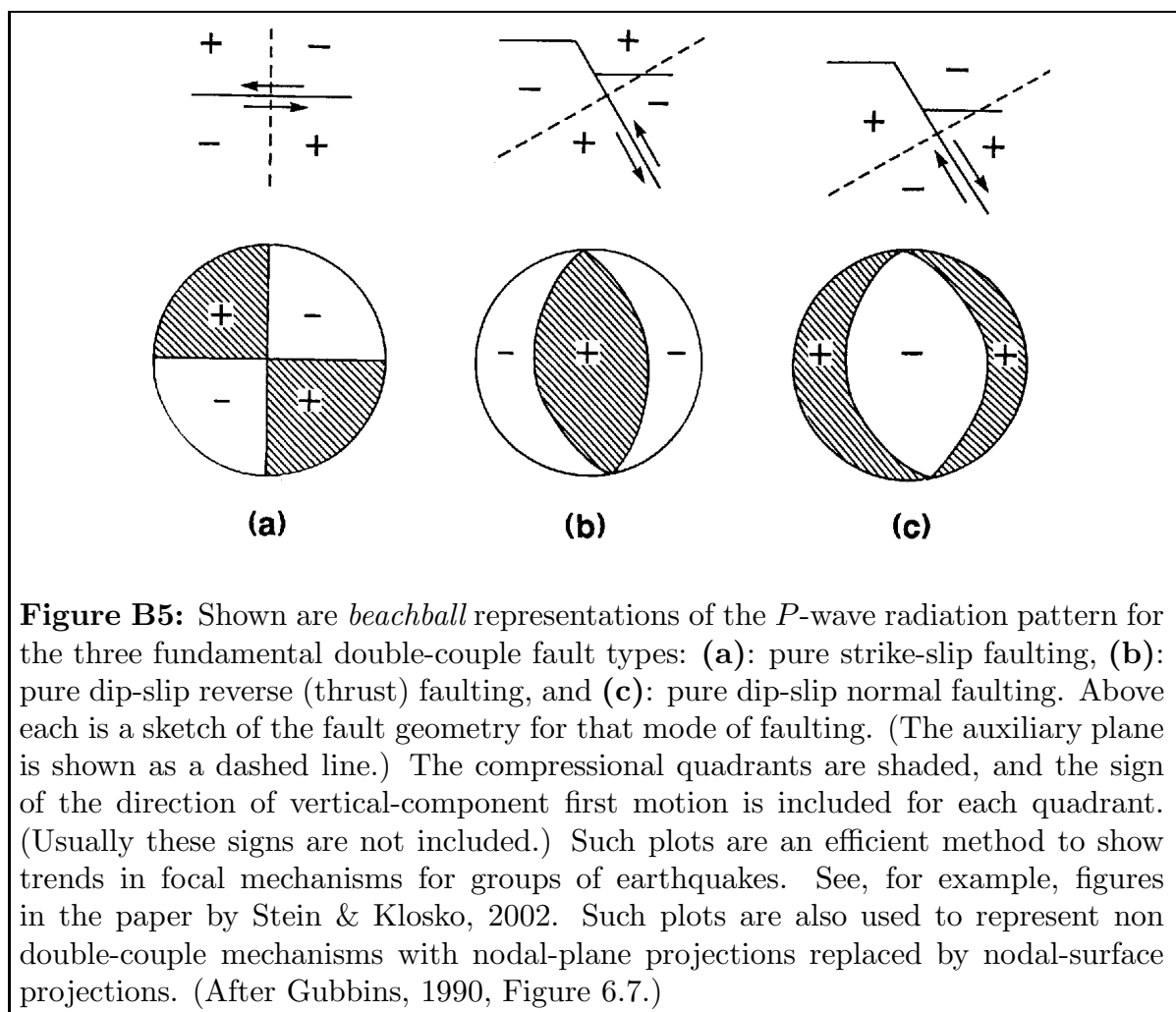
From Figure B4, one can see the basis for the polarity choices for station COR in the *Focmec* input files in subdirectory `./sample_runs/sakhalin`: D (down on *Vertical*) for *P*, B (down on *Radial*) for *SV*, and R (up on *Transverse*) for *SH*.

Upper- and Lower-Hemisphere Projections: The projections of the focal spheres shown above in Figures 1 and 2 are lower-hemisphere projections. This is the more popular projection, presumably because most data are teleseismically recorded. Some times an upper-hemisphere projection is used, so it is instructive to review briefly how these projections are related and how one constructs them.

The particle motion is identical for antipodal points on the focal sphere, so a projection (from above) of station positions and focal mechanism onto the upper hemisphere can be mapped onto the lower hemisphere by simply adding 180° to all station azimuths and trends for the **P** and **T** axes.

To get such plots, one projects the position on the focal sphere of the **P** and **T** axes (trends and plunges) and station polarities or amplitude ratios (takeoff angles and azimuths) onto a circle. For a station position, if it is an upper-hemisphere projection and the takeoff angle is up, the mapping is straightforward. If for that projection the takeoff angle is down, one maps the antipodal position onto the circle — the supplement of the takeoff angle and azimuth plus 180° . For a lower-hemisphere projection, the mapping is the opposite. It is easiest to derive the nodal surfaces from the directions of the **P** and **T** axes: As these axes project in antipodal directions from the focus, to map a lower-hemisphere vector into its upper-hemisphere counterpart, one simply adds 180° to the trend.

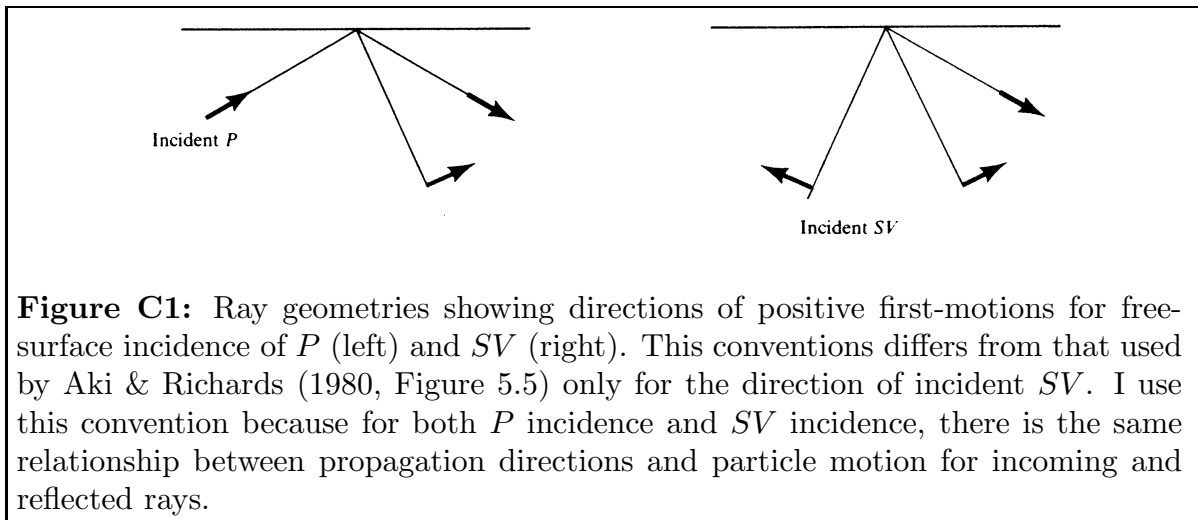
“Beachball” Representations of Focal Mechanisms



Appendix C: *SV* Polarities and Amplitudes Should be Used with Care

Kisslinger and coauthors (1980, 1981, 1982) describe procedures for using *SV/P* vertical-component amplitude ratios recorded by local and regional networks to constrain focal mechanisms. The emphasis was on the vertical components because at that time most networks used single-component seismographs and analog recording.

With modern instrumentation, one can often find well recorded *SV* arrivals — although generally not as well recorded as for the deep-focus Sakhalin Island event discussed above. We show below why *SV* should be used only with great care.



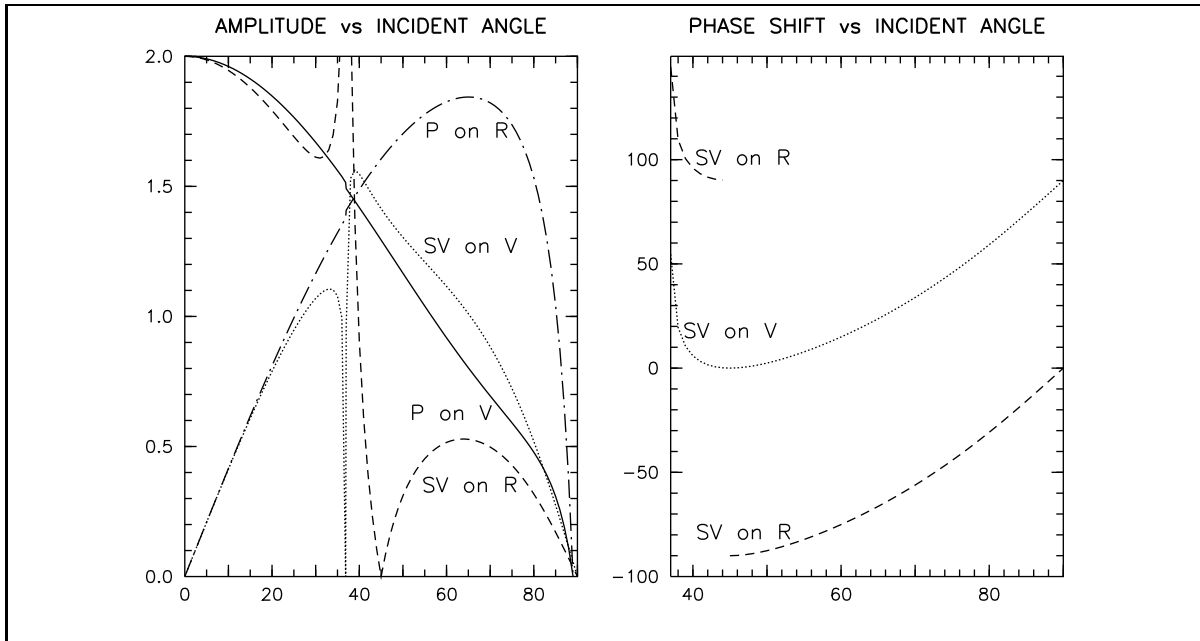


Figure C2: Free-surface amplitudes (left) and phase shift (right) for emergent *P* and *SV* at the free surface for a v_S/v_P ratio of 0.6. The critical angle is $\sin^{-1}(v_S/v_P) = 36.9^\circ$.

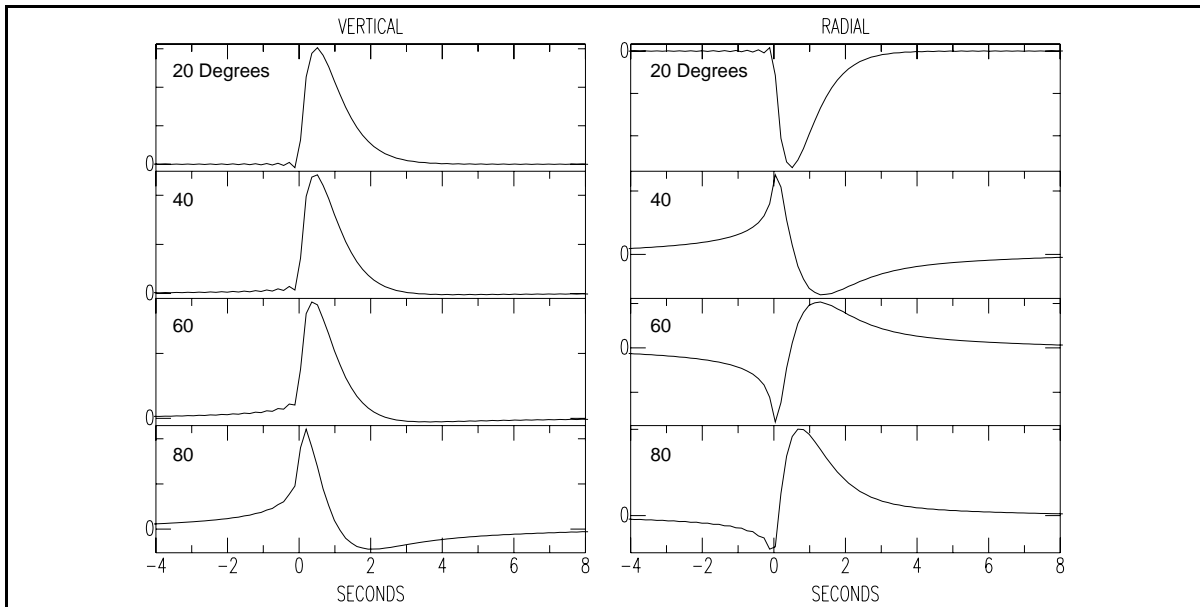


Figure C3: Waveforms for the vertical ground motion (left) and the radial ground motion (right) for planewave *SV* incidence angles of 20, 40, 60, and 80 degrees in a uniform halfspace with a v_S/v_P ratio of 0.6. Polarities follow the convention defined in Figure C1.

The input waveform for the ground motion shown in Figure C3 is normalized so that the area under the curve is the same as the amplitude for that component shown in Figure C2 when there is no phase shift. For P incidence, there is no critical angle and the polarities are all positive using the convention defined in Figure C1, so there is zero phase shift for all angles of incidence. The rest of this discussion is for SV incidence.

As discussed by Aki & Richards (1980, page 156), the sign of the “phase shift” depends on the Fourier sign convention and on the sign of the frequency. The phase shifts in Figure C2 use their conventions: positive frequencies and $+i\omega t$ for the forward Fourier transform. Because of the different polarity for SV incidence between them and Figure C1, phase shifts presented here will differ by 180° from theirs.

Below critical angle incidence, the phase shift is zero for the vertical ground motion and 180° for the radial motion (see waveforms for 20° incidence in Figure C3). At 45° incidence, the phase shift for the radial component jumps by 180° , which can be seen in the polarity flip between the waveforms on the radial component for 40° and 60° in Figure C3.

The rapid changes in amplitude within a few degrees of the critical angle mean that neither the vertical nor radial component amplitudes should be used for arrivals at those angles.

One sees from Figure B4 above that for small emergence angles (22° at COR for S for this event), SV is much better recorded on the radial than the vertical. In general, below about 30° SV on the radial component is the more reliable. For angles above the critical angle, the phase shift results in a drastic change in waveform for the radial component, so SV on the radial should definitely not be used in ratios and used only with great care for polarity.

For the vertical component with SV incidence, the polarity is stable up to about 80° , so those polarities can be used if the arrivals are well recorded. Up to about 50° , the small phase shift results in a negligible change in the amplitude, so the vertical component could be used in an amplitude ratio. At 80° , the waveform shown in Figure C3 is visibly changed and the amplitude is reduced to $0.27/0.52 = 0.52$ the amplitude predicted by the free-surface correction plotted in Figure C2.

Kisslinger *et al.* (1961) write that the free-surface correction for the SV/P ratio on the vertical, the free-surface correction is close to unity for incidence angles from a few degrees above the critical angle to about 80° . While that is true based on the amplitudes shown in Figure C2 (see also their Figure 1), the effect of the phase shifts on the waveforms and amplitudes leads to a much larger variation for higher angles.

The above discussion is based on planewave incidence — appropriate for teleseismically recorded events. In their paper on shear-wave polarization, Booth & Crampin (1985) show that for curved wavefronts associated with local to near-regional events, an SP arrival which comes in just before direct S affects the observed waveforms. In addition, a low-velocity zone at the surface can complicate the waveforms — particularly for SV incidence. Such considerations must also be considered when choosing polarities and amplitudes for focal mechanism determinations.